Crystal Structure and Luminescent Properties of Tb^{3+}, Ce^{3+}, and Codoped NaSrPO$_4$ Phosphors Prepared by Microwave Sintering

Kun-Hsien Chen, Min-Hang Weng,[1] Cheng-Tang Pan, and Ru-Yuan Yang[2*]

Department of Mechanical and Electro-Mechanical Engineering, National Sun Yat-Sen University,
Kaohsiung County 804, Taiwan
[1]Medical Devices and Opto-Electronics Equipment Department,
Metal Industries Research and Development Center, Kaohsiung County 811, Taiwan
[2]Graduate Institute of Materials Engineering, National Pingtung University of Science and Technology,
Pingtung County 912, Taiwan

A series of NaSr$_{1-x-y}$PO$_4$:xTb^{3+}:yCe^{3+} (x = 0.04) phosphors doped with Ce^{3+} at different concentrations were synthesized by microwave-assisted sintering. The crystal structure and luminescent properties of the phosphors were carefully investigated. X-ray diffraction (XRD) analysis confirmed that all the samples were matched with the standard patterns of NaSrPO$_4$, even though the doping concentrations of Ce^{3+} ions are increased to y = 0.07. All particles prepared by microwave-assisted sintering are very nearly spherical, except at the concentration of 0.07, at which they reveal a smooth and polygonal structure. The photoluminescence measurement shows that the major emission peak was located at 547 nm, approximating a green luminescence, which corresponds to a ^{5}D$_4$-to-^{7}F$_5$ transition, and the optimal Ce^{3+} concentration, which was 0.01, was observed. Moreover, the chromaticity (x, y) is changed with increasing Ce^{3+} concentration.

1. Introduction

There are many advantages of rare-earth (RE) ion-doped phosphates as phosphors applied in near-UV LEDs, such as superior color richness, and good chemical as well as thermal stability compared with non-oxide materials.[1] UV LEDs can generate warm white light and provide a highly efficient solid-state lighting compared with traditional common white-light LEDs (blue LED chip + yellow phosphor).

The phosphate series of phosphors with ABPO$_4$ [A (alkaline metals) and B (alkaline earth metals) are monovalent and divalent cations, respectively] compounds are considered to be ideal luminescent hosts. The rigid tetrahedral three-dimensional matrix of phosphate is considered to be ideal for charge stabilization, thus resulting in excellent thermal stability.[2] In the past, ABPO$_4$ compounds doped with different types of RE ions (Eu^{3+}, Ce^{3+}, Tb^{3+}, Sm^{3+}, etc.) were frequently reported in the literature,[3–5] wherein the Tb^{3+} and Ce^{3+} ions are two important RE ions used to generate green and blue emissions under UV excitation. Green-emitting phosphors such as LaPO$_4$[5] were obtained by utilizing a predominant ^{5}D$_4$→^{7}F$_5$ transition of Tb^{3+} ions at around

545 nm. A sensitizer is usually used to increase the absorption in the spectral range effectively. According to the Laporte parity selection rules, the Ce^{3+} ion may act as a highly efficient emission center owing to the allowed 4f–5d transitions. Ce^{3+} is a very good candidate sensitizer for the UV-emitting Tb^{3+} in such phosphate lattices.[6–8] Thus, many Ce^{3+} and Tb^{3+} codoped $ABPO_4$ phosphors have been reported and prepared, such as $NaBaPO_4$:Ce/Tb,[7,9] $NaCaPO_4$Ce/Tb,[8] and $LiZnPO_4$:Tb/Ce,[6] which encouraged us to think about the probability of the energy transfer between Ce^{3+} and Tb^{3+} in the $NaSrPO_4$ host. The phosphors required a long sintering time to synthesize using the solid-state reaction by conventional sintering.[10,11] However, using microwave energy as the source of the sintering process has been confirmed to improve the microstructure and properties of materials owing to different heating mechanisms.[12] Additionally, different host materials resulting in different crystal fields and different heating mechanisms providing different energy transfer methods of the phosphors could affect the fluorescent properties of the phosphor.[13] Novel host materials for codoping Tb^{3+} ions along with Ce^{3+} ions are important for the energy-transfer process. However, to the best of our knowledge, there are only a few reports on the research on $NaSrPO_4$:Ce^{3+} and Tb^{3+} for its potential application as a green phosphor. In a previous work, we investigated the microstructural and luminescence properties of the $NaSrPO_4$:Tb^{3+} phosphors with different Tb^{3+} concentrations prepared by microwave sintering.[14] The report indicates that the optimum doping concentration of Tb^{3+} for $NaSrPO_4$:Tb^{3+} phosphors is 0.04. Therefore, in this paper, we investigated and discussed the microstructure and luminescent properties of $NaSrPO_4$:Tb^{3+}:Ce^{3+} phosphors with different Ce^{3+} and fixed Tb^{3+} concentrations ($x = 0.04$) prepared by microwave sintering.

2.   Materials and Methods

The raw materials, Na_2CO_3, $SrCO_3$, $NH_4H_4PO_2$, Tb_4O_7, and Ce_2O_3 powders, all with a purity of 99.9%, were stoichiometrically weighed and dispersed in alcohol followed by ball milling for 3 h with zirconia balls. After drying, Tb^{3+}- and Ce^{3+}-doped $NaSr_{1-x-y}PO_4$:xTb^{3+}:yCe^{3+} ($x = 0.04$; $y = 0.005, 0.007, 0.01, 0.03, 0.05$, and 0.07) phosphors were synthesized by microwave-assisted sintering using a microwave furnace (Therm Wave Mod. III), with a continuously variable power of 2.45 GHz microwaves up to 1.3 kW.

Silicon carbide (SiC) was used as a susceptor to heat the powders indirectly due to the strong heating response to 2.45 GHz microwaves.[15] The material sample was placed in an Al_2O_3 crucible surrounded by four silicon carbide susceptors and encapsulated by a ceramic fiber insulating material in a microwave cavity. The mixed powders were sintered at 1200 °C for 3 h under an air atmosphere at 900 ± 20 W. The average heating rate of the microwave furnace was greater than 100 °C/min.

3.   Results and Discussion

3.1   Structure

Figure 1 shows the X-ray diffraction (XRD) results of the prepared $NaSr_{1-x-y}PO_4$:xTb^{3+}:yCe^{3+} phosphors with different Ce^{3+} concentrations ($x = 0.04$, $y = 0.005, 0.007, 0.01, 0.03, 0.05$, and 0.07). According to the Joint Committee on Powder Diffraction Standards (JCPDS, No. 33-1282) as a reference, all the samples are matched well with the standard patterns of $NaSrPO_4$, even though the
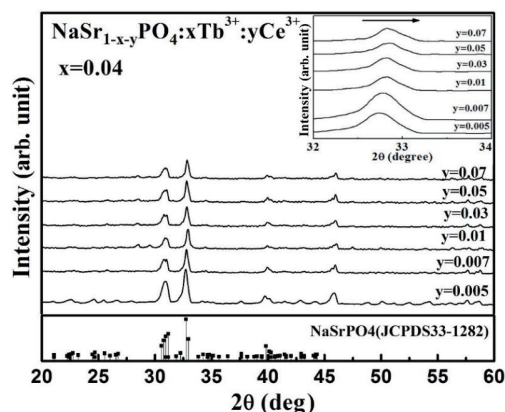
Fig. 1.   XRD results of the prepared $NaSr_{1-x-y}PO_4{:}xTb^{3+}{:}yCe^{3+}$ ($x = 0.04$) phosphors with various concentrations of Ce^{3+} ions.

doping concentration of Ce^{3+} ions is increased to $x = 0.07$. That is, the site of Sr^{3+} ions in $NaSrPO_4$ phosphate can be easily replaced by Tb^{3+} and Ce^{3+} ions to form a solid solution, because Sr^{2+} can be replaced by RE (RE = Eu^{2+}, Eu^{3+}, Sm^{3+}, Tb^{3+}, etc.) owing to its large size to achieve full-color luminescence.[16] In addition, the JCPDS cards indicate that the $NaSrPO_4$ host material has a standard monoclinic crystal structure in which the lattice parameters have lengths $a = 2.041$ nm, $b = 0.543$ nm, $c = 1.725$ nm, and an angle $\beta = 101.76°$.[17,18]

The inset of Fig. 1 shows the enlargement of the main diffraction peak with various concentrations of Ce^{3+} ions. The main diffraction peak shifts slightly toward the higher angle direction (32.75 to 32.84°) as the Ce^{3+} concentration increases because the ion radii of Ce^{3+} (1.14 Å) and Tb^{3+} (1.04 Å) are smaller than that of Sr^{2+} (1.29 Å). The result indicates that the ion radii mismatch would cause crystal lattice distortion.[14] In addition, the full width at half maximum (FWHM) of the X-ray diffraction peak from Scherrer's equation could be used to calculate the average crystal size (D) as given by Eq. (1).

$$D = 0.9\lambda/\omega \cos\theta, \tag{1}$$

where ω is the calibrated FWHM of the selected diffraction line in radians, θ is the Bragg angle, and λ is the X-ray wavelength (0.15406 nm). The crystal size (D) of the $NaSr_{1-x-y}PO_4{:}xTb^{3+}{:}yCe^{3+}$ ($x = 0.04$; $y = 0.005, 0.007, 0.01, 0.03, 0.05,$ and 0.07) phosphor by microwave-assisted sintering was calculated and listed in Table 1. With increasing Ce^{3+} ion concentration, there is no obvious impact on the crystal size of the $NaSr_{1-x-y}PO_4{:}xTb^{3+}{:}yCe^{3+}$ phosphors.

3.2   Morphology

Figure 2 shows typical SEM images of the prepared $NaSr_{1-x-y}PO_4{:}xTb^{3+}{:}yCe^{3+}$ phosphors ($x = 0.04$; $y = 0.005, 0.007, 0.01, 0.03, 0.05,$ and 0.07). When the Ce^{3+} doping concentrations were at $y = 0.005$, 0.007, and 0.01, the average particle sizes were estimated in the range of 3–7 μm. When the values were at $y = 0.03, 0.05,$ and 0.07, the average particle sizes were estimated in the range of 6–10 μm. Although the concentration of Ce^{3+} ions had no obvious impact on the crystal size of

Table 1
Average crystal size (D) and color coordinates (CIE) of the prepared $NaSr_{1-x-y}PO_4$:xTb^{3+}:yCe^{3+} phosphors with different Ce^{3+} concentrations ($x = 0.04$, $y = 0.005$, 0.007, 0.01, 0.03, 0.05, and 0.07).

Ce^{3+} Concentration (y)	0.005	0.007	0.01	0.03	0.05	0.07
Crystal size (D) (nm)	26.8	26.5	26.4	26.9	27.4	27
CIE (x, y)	(0.21, 0.23)	(0.22, 0.23)	(0.30, 0.53)	(0.30, 0.52)	(0.27, 0.44)	(0.29, 0.55)

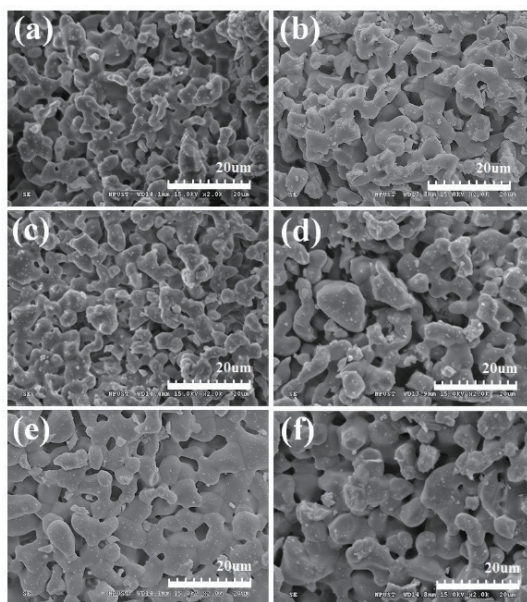Fig. 2.   SEM images of the prepared $NaSr_{1-x-y}PO_4$:xTb^{3+}:yCe^{3+} ($x = 0.04$) phosphors with various concentrations of Ce^{3+} ions at (a) $y = 0.005$, (b) $y = 0.007$, (c) $y = 0.01$, (d) $y = 0.03$, (e) $y = 0.05$, and (f) $y = 0.07$.

the $NaSr_{1-x-y}PO_4$:xTb^{3+}:yCe^{3+} phosphors, the particles show high aggregation, fragmentation, and slight growth when the concentration of Ce^{3+} ions is increasing. The Ce^{3+} and Tb^{3+} ions were diffused into the $NaSrPO^4$ phases readily during the calcine processes. When the concentrations of Ce^{3+} and Tb^{3+} ions increase continuously, the limit effect of the seeds will be weakened resulting in the natural growth of the phosphor particles.[19]

3.3   Excitation and emission spectra

Figure 3(a) shows the excitation spectrum monitored at 547 nm of the prepared $NaSr_{1-x-y}PO_4$:xTb^{3+}:yCe^{3+} ($x = 0.04$) phosphors with various concentrations of Ce^{3+} ions. Several peaks in the spectral region from 200 to 400 nm are associated with the f–f and f–d transitions of Tb^{3+} and Ce^{3+} ions. The strongest peak intensity was located at 229 nm and the maximum value was obtained as the concentration of the Ce^{3+} ion is $y = 0.01$, and then decreases with the increase in the Ce^{3+} concentration. The weaker peak intensity in the spectral region from 350 to 390 nm belonged to electronic-dipole-forbidden f–f transitions of the Tb^{3+} ions.[6] The Gaussian multipeak fit of the excitation spectrum of the Tb^{3+}/Ce^{3+}-doped sample is shown in the inset of Fig. 3(a). There were two Gaussian emission bands fitted into the peaks at 229 nm, which belonged to the common absorption bands of Tb^{3+} ($^7F_6{\rightarrow}^5I_6$) and Ce^{3+} ($^2F_{5/2}{\rightarrow}^5d$). One centered at 223 nm [Ce^{3+} ($^2F_{5/2}{\rightarrow}^5d$)], and the other peak centered at 231 nm [Tb^{3+}($^7F_6{\rightarrow}^5I_6$)].[7] However, the wavelength of the excitation peak is 229 nm, which is slightly shorter than the peak of 266 nm

Fig. 3.   (a) Excitation spectra and (b) emission spectra of the prepared $NaSr_{1-x-y}PO_4:xTb^{3+}:yCe^{3+}$ ($x = 0.04$) phosphor with various concentrations of Ce^{3+} ions. The inset of Fig. 3(b) shows the emission intensity at the wavelength of 546 nm from various concentrations of Ce^{3+} ions.

reported by Cheng *et al.*[1] A sensitizer is used to transfer the excitation energy to the RE activator by exciting an optically allowed transition resulting in high light output. A well-known example is the sensitizer of Ce^{3+} from the broad to the narrow-line Tb^{3+} activator due to the nearest neighbors in the crystal lattice and optimal spectral overlap.[20] However, the structure of $NaSrPO_4$ is related to the β-K_2SO_4 type and belongs to the monoclinic system. Therefore, $NaSrPO_4$ has three different Na sites (Na1, Na2, and Na3) and three different Sr sites (Sr1, Sr2, and Sr3) in the lattices in comparison with the same β-K_2SO_4 type structure of $KBaPO_4$, which belongs to the orthorhombic system.[21] In such disordered multisite structure of $NaSrPO_4$ codoped with Ce^{3+}/Tb^{3+} ions, the excitation energy could distribute in a different way from the various sites so that the excited range would be affected owing to the different host structure surrounding the Tb^{3+}/Ce^{3+}.

Figure 3(b) shows the emission spectra of the prepared $NaSr_{1-x-y}PO_4:xTb^{3+}:yCe^{3+}$ ($x = 0.04$) phosphors with various concentrations of Ce^{3+} ions. There are six emission transitions in the range of 400–650 nm, and the strongest emission band is located at 546 nm ($^5D_4 \rightarrow {}^7F_5$). The emission peaks originate from $^5D_3 \rightarrow {}^7F_J$ ($J = 4, 5$) such as $5D_3 \rightarrow 7F_5$ (418 nm) and $^5D_3 \rightarrow {}^7F_4$ (440 nm), and $^5D_4 \rightarrow {}^7F_J$ ($J = 3, 4, 5, 6$) such as $^5D_4 \rightarrow {}^7F_6$ (493 nm), $^5D_4 \rightarrow {}^7F_5$ (547 nm), $^5D_4 \rightarrow {}^7F_4$ (587 nm), and $^5D_4 \rightarrow {}^7F_3$ (625 nm). The emissions of $^5D_3 \rightarrow {}^7F_J$ ($J = 4, 5$) transitions are much weaker than those of $^5D_4 \rightarrow {}^7F_J$ ($J = 3, 4, 5, 6$), owing to cross-relaxation, which is a one-step transfer of part of the energy from excited donors to acceptors.[7,14] The emission spectrum of the Tb^{3+}/Ce^{3+}-doped phosphor consists of two parts. One is the weak blue emission below the wavelength of 450 nm, originating from the relaxation of the $^5D_3 \rightarrow {}^7F_J$ ($J = 4, 5$) transitions. The other is the strong yellowish green and red emissions above the wavelength of 450 nm, originating from the relaxation of the $^5D_4 \rightarrow {}^7F_J$ ($J = 3, 4, 5, 6$) transitions. The intensity at the wavelength of 547 nm from the $^5D_4 \rightarrow {}^7F_5$ transition was slightly increased by changing the codoping concentration of the Ce^{3+} ion. It is difficult to distinguish the peak intensity contributed by the Ce^{3+} or Tb^{3+} due to overlap.[22]

The inset of Fig. 3(b) shows the emission intensity at the wavelength of 547 nm obtained from various concentrations of Ce^{3+} ions. It reaches a maximum value when the concentration of the Ce^{3+} ion is 0.01 and then concentration quenching occurred. When the activator and sensitizer occupy adjacent lattice sites, the wave functions of the sensitizer and activator could overlap to exchange electronics, and then the mechanism of exchange interaction could be induced by the energy transfer.[14]

The mechanism of energy transfer was proposed by Blasse[23] and calculated using the concentration quenching method describing the critical energy transfer distance (R_C). R_C for energy transfer between the host lattice, activator, and sensitizer and the critical distance was estimated as[24]

$$R_C \approx 2\left(\frac{3V}{4\pi X_C N}\right)^{1/3},$$ (2)

where V is the volume of the unit cell, X_C is the total concentration of Tb^{3+} and Ce^{3+} ions, and N is the number of formula unit per unit cell. For the $NaSrPO_4$ host, $N = 16$, $X_C = 0.05$, 0.04 (without Ce^{3+} ion), and $V = 1.87121$ nm^3. According to Eq. (2), the critical distance (R_C) of the $NaSr_{1-x-y}PO_4{:}xTb^{3+}{:}yCe^{3+}$ ($x = 0.04$, $y = 0.01$) phosphor was calculated to be about 1.65 nm, which is less than that obtained without Ce^{3+} ion doping (1.77 nm). The critical distance between the activator and the sensitizer becomes smaller as the concentration of Ce^{3+} ions was increased owing to the overlap of the wave functions of the sensitizer and activator. Moreover, according to Dexter's theory, the energy transfer mechanism resulted from the nonradioactive interaction among the activator and the sensitizer.[25]

3.4 Commission International de l'Eclairage (CIE) 1931 chromaticity

In general, color can be expressed by means of color coordinates and the CIE 1931, which is a two-dimensional graphical representation of any color perceptible by the human eye on an x–y plot. Therefore, all the results calculated from Fig. 3(b) were drawn in the CIE 1931 chromaticity diagram as shown in Fig. 4. The chromaticity (x, y) is changed with increasing Ce^{3+} concentration and the values are listed in Table 1.

The result indicates that the chromaticity coordinates of the $NaSr_{1-x-y}PO_4{:}xTb^{3+}{:}yCe^{3+}$ ($x = 0.04$) phosphors with various concentrations of Ce^{3+} ions have a very large shift range from blue to green. Therefore, by tuning the Ce^{3+} doping concentration, the $NaSr_{1-x-y}PO_4{:}xTb^{3+}{:}yCe^{3+}$ ($x = 0.04$) phosphors could have different color applications.
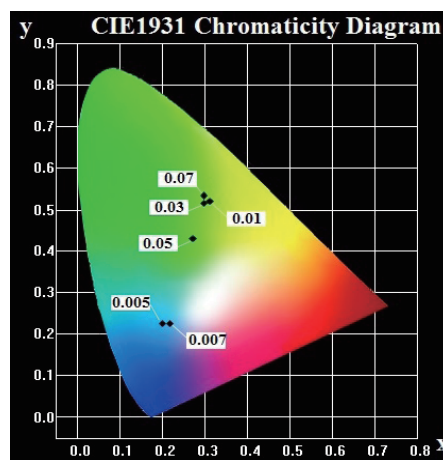

Fig. 4.   (Color online) CIE 1931 chromaticity diagram of the prepared $NaSr_{1-x-y}PO_4{:}xTb^{3+}{:}yCe^{3+}$ ($x = 0.04$) phosphors with various concentrations of Ce^{3+} ions.

4. Conclusions

In summary, we have successfully synthesized $NaSr_{1-x-y}PO_4:xTb^{3+}:yCe^{3+}$ ($x = 0.04$; $y = 0.005$, 0.007, 0.01, 0.03, 0.05, and 0.07) phosphors using microwave sintering at 1200 °C for 3 h in air atmosphere. The XRD results showed that with increasing doping concentration of the Ce^{3+} ions, the crystal structure of $NaSrPO_4$ does not change and remains to be a single phase, but the diffraction peak shifts slightly toward the higher angle direction (32.75 to 32.84°) owing to the smaller Ce^{3+} and Tb^{3+} ion radii than that of Sr^{2+}. With increasing Ce^{3+} ion concentration, there is no obvious impact on the crystal size of the $NaSr_{1-x-y}PO_4:xTb^{3+}:yCe^{3+}$ phosphors from the XRD results. However, the particles show high aggregation, fragmentation, and slight growth when the concentration of the Ce^{3+} ions is increasing because the limit effect of the seeds will be weakened resulting in the natural growth of the phosphor particles during the calcine processes. Owing to the disordered multisite structure of $NaSrPO_4$ codoped by Ce^{3+}/Tb^{3+} ions, the excitation energy could distribute in a different way from the various sites so that the wavelength of the excitation peak of the $NaSr_{1-x-y}PO_4:xTb^{3+}:yCe^{3+}$ phosphor is also located in the UV range, and not to transfer the excitation energy to the Tb^{3+} activator by exciting an optically allowed transition of Ce^{3+}. As $NaSr_{1-x-y}PO_4:xTb^{3+}:yCe^{3+}$ phosphors were excited at 229 nm, the highest emission peak intensities were located at 547 nm as the concentration of Ce^{3+} was increased to 0.01 and then concentration quenching occurred. Moreover, the calculated R_C value was approximately 1.65 nm and became smaller as the concentration of Ce^{3+} ions was increased owing to the overlap of the wave functions of the sensitizer and activator from the nonradiative energy transfer mechanism, thereby improving the photoluminescence properties of the $NaSrPO_4:Tb^{3+}$ phosphor. Finally, the chromaticity (x, y) is changed with increasing Ce^{3+} concentration. Therefore, by tuning the Ce^{3+} doping concentration, the $NaSr_{1-x-y}PO_4:xTb^{3+}:yCe^{3+}$ ($x = 0.04$) phosphors could have different color applications.

References

1 S. D. Cheng, C. H. Kam, and S. Buddhudu: Mater. Res. Bull. **36** (2001) 1131.
2 Y. K. Su, Y. M. Peng, R. Y. Yang, and J. L. Chen: Opt. Mater. **34** (2012) 1598.
3 Z. C. Wu, J. Liu, and M. L. Gong: Chem. Phys. Lett. **466** (2008) 88.
4 Z. P. Yang, G. W. Yang, S. L. Wang, J. Tian, X. N. Li, Q. L. Guo, and G. S. Fu: Mater. Lett. **62** (2008) 1884.
5 V. Pankratov, A. I. Popov, A. Kotlov, and C. Feldmann: Opt. Mater. **33** (2011) 1102.
6 C. M. Ouyang, S. Ma, Y. Rao, X. M. Zhou, X. Z. Zhou, and Y. X. Li: J. Rare Earth **30** (2012) 637.
7 J. Y. Sun, X. Y. Zhang, Z. G. Xia, and H. Y. Du: J. Electrochem. Soc. **158** (2011) J368.
8 N. Guo, Y. H. Song, H. P. You, G. A. Jia, M. Yang, K. Liu, Y. H. Zheng, Y. J. Huang, and H. J. Zhang: Eur. J. Inorg. Chem. **29** (2010) 4636.
9 X. H. Dou, W. R. Zhao, E. H. Song, L. L. Deng, X. B. Fang, and H. C. Min: J. Rare Earth. **30** (2012) 739.
10 J. Dhanaraj, R. Jagannathan, T. R. N. Kutty, and C. H. Lu: J. Phys. Chem. B **105** (2001) 11098.
11 W. J. Park, M. K. Jung, T. Masaki, S. J. Im, and D. H. Yoon: Mater. Sci. Eng. B **146** (2008) 95.
12 R. Y. Yang, H. Y. Chen, C. M. Hsiung, and S. J. Chang: Ceram. Int. **37** (2011) 749.
13 Y. M. Peng, Y. K. Su, and R. Y. Yang: Proc. 2012 Active-Matrix Flatpanel Displays and Devices Conf. (AM-FPD '12) p. 87.

14 K. H. Chen, M. H. Weng, C. T. Pan, and R. Y. Yang: Powder Technol. **288** (2016) 117.
15 P. D. Ramesh, D. Brandon, and L. Schachter: Mater. Sci. Eng. A **266** (1999) 211.
16 C. C. Lin, R. S. Liu, Y. S. Tang, and S. F. Hu: J. Electrochem. Soc. **155** (2008) J8.
17 Y. L. Tung and J. H. Jean: J. Am. Ceram. Soc. **92** (2009) 1860.
18 R. Y. Yang, C. T. Pan, K. H. Chen, and C. Y. Hung: Opt. Mater. **35** (2013) 2183.
19 Y. Pu, K. Tang, D. C. Zhu, T. Han, C. Zhao, and L. L. Peng: Nano-Micro Lett. **5** (2013) 117.
20 M. T. Jose and A. R. Lakshmanan: Opt. Mater. **24** (2004) 651.
21 S. Zhang, Y. Nakai, T. Tsuboi, Y. Huang, and H. J. Seo: Inorg. Chem. **50** (2011) 2897.
22 K. Y. Jung and H. W. Lee: J. Lumin. **126** (2007) 469.
23 G. Blasse: Philips Res. Rep. **24** (1969) 131.
24 Z. C. Wu, J. X. Shi, J. Wang, and M. L. Gong: J. Solid State Chem. **179** (2006) 2356.
25 D. L. Dexter: J. Chem. Phys. **21** (1953) 836.

About the Authors

Kun-Hsien Chen received his B.S. and M.S. degrees from Kun Shan University, Taiwan, in 2007 and 2009, respectively, and his Ph.D. degree from National Sun Yat-Sen University, Taiwan, in 2016. His research interests are in LED phosphors and solar cells.

Min-Hang Weng received his B.S., M.S., and Ph.D. degrees from National Cheng Kung University, Taiwan, in 1994, 1996, and 2000, respectively. From 2000, he was a researcher at a legal foundation in Taiwan. His research interests are in RF filters, solar cells, and LED phosphors.

Cheng-Tang Pan received his M.S. and Ph.D. degrees from National Tsing Hua University, Taiwan, in 1993 and 1998, respectively. Since 2008, he has been a professor at National Sun Yat-Sen University, Taiwan. His research interests are in MEMS, LIGA-like processes, and LED phosphors.

Ru-Yuan Yang received her B.S. degree from National Taiwan Normal University, Taiwan, in 1996, her M.S. degree from National Sun Yat-Sen University, Taiwan, in 2000, and her Ph.D. degree from National Cheng Kung University, Taiwan, in 2007. Since 2014, she has been a professor at National Pingtung University of Science and Technology, Taiwan. Her research interests are in LED phosphors, solar cells, and semiconductor processes.